Kinetic Study of Methacrylate Copolymerization Systems by Thermoanalysis Methods

Ali Habibi,[1] Ebrahim Vasheghani-Farahani[2]

[1]*Chemical Engineering Department, University of Tehran, P.O. Box 11365-4563, Tehran, Iran*
[2]*Chemical Engineering Department, Tarbiat Modares University, P.O. Box 14115-143, Tehran, Iran*

Received 16 April 2007; accepted 29 December 2007
DOI 10.1002/app.28243
Published online 27 May 2008 in Wiley InterScience (www.interscience.wiley.com).

ABSTRACT: The free-radical solution copolymerization of isobutyl methacrylate with lauryl methacrylate in the presence of an inhibitor was studied with thermoanalysis methods. A set of inhibited polymerization experiments was designed. Four different levels of initial inhibitor/initiator molar ratios were considered. *In situ* polymerization experiments were carried out with differential scanning calorimetry. Furthermore, to determine the impact of the polymerization media on the rate of initiation, the kinetics of the initiator decomposition were followed with nonisothermal thermoanalysis methods, and the results were compared with *in situ* polymerization counterparts. The robust *M*-estimation method was used to retrieve the kinetic parameters of the copolymerization system. This estimation method led to a reasonable prediction error for the dataset with strong multicollinearity. The model-free isoconversional method was employed to find the variation of the Arrhenius activation energy with the conversion. It was found that robust *M*-estimation outperformed existing methods of estimation in terms of statistical precision and computational speed, while maintaining good robustness. © 2008 Wiley Periodicals, Inc. J Appl Polym Sci 109: 3302–3314, 2008

Key words: copolymerization; differential scanning calorimetry (DSC); modeling; radical polymerization; thermogravimetric analysis (TGA)

INTRODUCTION

The interpretation of polymerization kinetics demands knowledge of reliable kinetic parameters. They provide the basis for more accurate design of polymerization reactors and better insight into the behavior of existing reactors. Recent studies have shown that the copolymer of isobutyl methacrylate (i-BMA) and lauryl methacrylate (LMA) is an important multifunctional oil additive with several functions, such as viscosity-index improver, pour point depressant, and sludge dispersant.[1] Still, to the best of our knowledge, the kinetics of this copolymerization system have not been studied with thermoanalysis methods. Furthermore, in free-radical polymerization with thermal initiators, thermoanalysis methods help us to find the temperature at which enough radicals are formed to initiate the reaction efficiently. Although the literature contains an abundance of initiator decomposition rates in various solvents,[2] the *in situ* rate data for polymerization systems are scarce.

Different thermoanalysis methods, such as thermogravimetry (TG), differential thermal analysis, differential scanning calorimetry (DSC), and thermovolumetry, have been used for kinetic studies of reacting systems.[3] The results of these experiments are usually represented by a curve, the features of which (peaks, discontinuities, changes in slope, etc.) can be related to the thermal events in the sample. Nonisothermal thermoanalysis methods[4] have some advantages over isothermal methods: (1) the dependence of the heat generation rate on temperature can be determined over a wide temperature range by a single experiment and (2) the continuous recording of heat and weight losses versus temperature ensures that no features of the reaction are overlooked.

DSC has found several applications in the determination of the reaction kinetics, degree of crystallinity, melting point, material purity, and glass-transition temperature of polymers.[3] Although polymerization reactions are highly exothermic, in the case of complex energetic reactions, kinetic analysis based on DSC data needs some consideration; the peaks may be a balance among exothermic and endothermic events, and so the kinetic evaluations may be problematic. The application of DSC to the kinetic study of homopolymerization was developed by Horie[5] as well as other investigators.[6,7] The application of DSC to the kinetic studies of copolymerization systems is less clear-cut. Horie successfully applied the DSC method to copolymerization

Correspondence to: E. Vasheghani-Farahani (evf@modares.ac.ir).

© 2008 Wiley Periodicals, Inc.

systems in which the two comonomers have equal heats of reaction. Thus, the heat of copolymerization was assumed to be constant and independent of the monomer composition. It has also been shown that complex copolymerization kinetics can be accurately approximated by a simple lumped kinetic model of enthalpy, provided that one of the comonomers is not totally consumed before the completion of the reaction.[6] The lumped kinetic model defines a heat of reaction that is dependent on the initial feed composition but does not vary with compositional drift during the course of polymerization. In fact, in copolymerization systems, the heat of reaction varies with the conversion because of compositional drift, preventing the simple reduction of calorimetric data to rate data.

To retrieve the kinetic parameters of thermal reactions, a couple of model-fitting[8–18] and model-free[19–25] kinetic methods have been presented in the literature. The model fitting methods suffer from the inability to uniquely determine the reaction model. This shortcoming does not allow reliable mechanistic conclusions to be made even from isothermal data. Model-free methods help us to avoid the problems that originate from the uncertainty of the reaction model and allow us to determine the dependence of the activation energy on the conversion.

The robust *M*-estimator is a widely used statistical method because of its robustness with respect to outliers[26,27] and low computational effort. Its major benefit over other techniques is mainly apparent if it is applied to datasets consisting of blocks of variables subject to problems such as multicollinearity. Huber[28] introduced the class of *M*-estimators that have good efficiency properties over a wide range of error distributions. It has been shown that for many types of error distributions, the robust *M*-estimator outperforms the least square estimator in terms of efficiency, resulting in smaller prediction errors.[29]

THEORETICAL BACKGROUND

Inhibited polymerization

Kinetic modeling of copolymerization systems is subject to the variability of the rate parameter values, which are usually both composition- and conversion-dependent. In general, by the use of the pseudokinetic rate constant (PKRC) method,[30] the kinetic treatment of a multicomponent polymerization can be reduced to that of homopolymerization.[31,32] This method can be applied to chain statistics based on a terminal unit model as well as higher order Markov chain statistics such as a penultimate unit model. On the basis of the PKRC method, the inhibited free-radical copolymerization can be adequately represented by the following kinetic scheme:

$$\text{Initiation}: \begin{cases} \mathrm{I} \xrightarrow{\bar{k}_d} 2\mathrm{R}^\bullet \\ \mathrm{R}^\bullet + \mathrm{M} \xrightarrow{\bar{k}_i} \mathrm{P}_1^\bullet \end{cases} \quad (1\text{-}1)$$

$$\text{Primary radical inhibition}: \ \mathrm{P}_1^\bullet + \mathrm{Z} \xrightarrow{\bar{k}_z} \mathrm{P}_1 + \mathrm{Z}^\bullet \quad (1\text{-}2)$$

$$\text{Propagation}: \ \mathrm{P}_{n-1}^\bullet + \mathrm{M} \xrightarrow{\bar{k}_p} \mathrm{P}_n^\bullet \quad (1\text{-}3)$$

$$\text{Inhibition or retardation}: \ \mathrm{P}_n^\bullet + \mathrm{Z} \xrightarrow{\bar{k}_z} \mathrm{P}_n + \mathrm{Z}^\bullet \quad (1\text{-}4)$$

$$\text{Reinitiation}: \mathrm{Z}^\bullet + \mathrm{M} \xrightarrow{\bar{k}_{zp}} \mathrm{P}_1^\bullet \quad (1\text{-}5)$$

$$\text{Annihilation reaction}: \ 2\mathrm{Z}^\bullet \xrightarrow{\bar{k}_{zt}} \begin{cases} \mathrm{Z}_2 \\ \mathrm{Z}^{\|} + \mathrm{Z} \end{cases} \quad (1\text{-}6)$$

$$\text{Combination}: \ \mathrm{P}_n^\bullet + \mathrm{P}_m^\bullet \xrightarrow{\bar{k}_{tc}} \mathrm{P}_{n+m} \quad (1\text{-}7)$$

$$\text{Disproportionation}: \mathrm{P}_n^\bullet + \mathrm{P}_m^\bullet \xrightarrow{\bar{k}_{td}} \mathrm{P}_n + \mathrm{P}_m \quad (1\text{-}8)$$

$$\text{Transfer to solvent}: \mathrm{P}_n^\bullet + \mathrm{S} \xrightarrow{\bar{k}_{tr}} \mathrm{P}_n + \mathrm{P}_1^\bullet \quad (1\text{-}9)$$

where I is the initiator, $R^\bullet$ is the primary radical, M is the monomer, Z is the inhibitor, $Z^\bullet$ is the inhibitor radical, S is the solvent, $P_i^\bullet$ is the polymer molecule with length i, and $P_i^\bullet$ is the radical with length i.

The pseudokinetic values of the decomposition, initiation, propagation, inhibition, termination. and transfer rate parameters are denoted by $\bar{k}_d$, $\bar{k}_i$, $\bar{k}_p$, $\bar{k}_z$, $\bar{k}_t$, and $\bar{k}_{tr}$, respectively. $\bar{k}_{td}$ is the termination by disproportionation rate parameter, $\bar{k}_{tc}$ is the termination by combination rate parameter, $\bar{k}_{zp}$ is the reinitiation rate parameter, and $\bar{k}_{zt}$ is the annihilation rate parameter. These parameters are functions of conversion due to compositional drift and can be estimated from the conversion and/or molecular weight data. In addition to composition and conversion dependence, the inhibition parameter ($\bar{k}_z/\bar{k}_p$) varies considerably with the reactivity and polarity of the propagating radicals.

Methacrylate monomers are highly reactive. To avoid gel and viscosity effects and solubility problems in the early stages of polymerization, the inhibited polymerization system is studied. Inhibitors react with the initiating and propagating radicals, converting them into either nonradical species or radicals of very low reactivity to undergo propagation. The stable free radical 2,2-diphenyl picryl hydrazyl (DPPH) is a powerful inhibitor for the polymerization of either monomer, but its inhibition efficiency is highly sensitive to the presence of dissolved oxygen.[7] In typical polymerization systems, the monomer concentration is about 10^4 times the

inhibitor concentration, and the propagation constant of primary radicals toward the monomer is about 10^{-2} to 10^{-3} times of the reaction with the inhibitor. Therefore, it is expected that most of the primary radicals will react with the inhibitor. Some investigators have used inhibitors in polymerization experiments to establish an initial baseline for thermoanalysis curves. In this study, to get more reliable kinetic parameters for the polymerization system, the reactions were conducted to low conversion levels. On the basis of the kinetic scheme in eqs. (1-1)–(1-9), the population balance for live and dead species can be written as follows:

$$\frac{d[\mathrm{I}]}{dt} = -\bar{k}_d[\mathrm{R}^\bullet]^2 \tag{2-1}$$

$$\frac{d[\mathrm{M}]}{dt} = -(\bar{k}_i[\mathrm{R}^\bullet] + \bar{k}_p[\mathrm{P}_{n-1}^\bullet] + \bar{k}_{zp}[\mathrm{Z}^\bullet])[\mathrm{M}] \tag{2-2}$$

$$\frac{d[\mathrm{Z}]}{dt} = -\bar{k}_z[\mathrm{P}_n^\bullet][\mathrm{Z}] + \varsigma\bar{k}_{zt}[\mathrm{Z}^\bullet]^2 \tag{2-3}$$

$$\frac{d[\mathrm{P}_n^\bullet]}{dt} = R_i - \bar{k}_z[\mathrm{P}_n^\bullet][\mathrm{Z}] - 2\bar{k}_t[\mathrm{P}_n^\bullet]^2 + \bar{k}_{zp}[\mathrm{Z}^\bullet][\mathrm{M}] \tag{2-4}$$

$$\frac{d[\mathrm{Z}^\bullet]}{dt} = \bar{k}_z[\mathrm{P}_n^\bullet][\mathrm{Z}] - \bar{k}_{zp}[\mathrm{Z}^\bullet][\mathrm{M}] - 2\bar{k}_{zt}[\mathrm{Z}^\bullet]^2 \tag{2-5}$$

where [I] is the initiator concentration (mol/L). Parameter ζ in eq. (2-3) changes between 0 and 1. If in eq. (1-6) annihilation dominates, ζ is equal to 0, and if the disproportionation reaction proceeds with the release of an inhibitor molecule, ζ is equal to unity. During the induction period, the steady-state hypothesis for radicals ($d[\mathrm{P}_n^\bullet]/dt = 0$; $d[\mathrm{Z}^\bullet]/dt = 0$) is a reasonable assumption, and the inhibition reaction dominates bimolecular termination:

$$\frac{d[\mathrm{z}]}{dt} = -\left(1 - \frac{\varsigma}{2}\right)R_i - \bar{k}_{zp}\left(\frac{R_i}{2\bar{k}_{zt}}\right)^{0.5}[\mathrm{M}] \tag{3}$$

where R_i is the initiation rate (mol/L min) and [M] is the overall monomer concentration (mol/L). If $k_{zp} \cong 0$, the second right-hand term in eq. (3) vanishes, and during the inhibition period

$$[\mathrm{Z}] = [\mathrm{Z}]_0 - \left(1 - \frac{\varsigma}{2}\right)R_i t \tag{4}$$

where t is the polymerization time. Then, by some mathematical manipulations of eqs. (2) and (4), the rate of monomer consumption can be obtained as follows:

$$\frac{1}{1-X}\frac{dX}{dt} = \frac{1}{\overline{C}_z\left[\left(\frac{[\mathrm{Z}]_0}{[\mathrm{I}]_0}\right)\frac{e^{\bar{k}_d t}}{2f\bar{k}_d} - \frac{t}{\Omega}\right]} \tag{5}$$

where X is the overall conversion, $\overline{C}_Z$ is the inhibition parameter, f is the initiator efficiency, and Ω is a physical parameter defined as $1/(1 - \zeta/2)$, which is equal to the number of terminated radicals per each molecule of the inhibitor.

After the inhibition period, the overall copolymerization rate is simply obtained by the PKRC method in a way similar to that for uninhibited homopolymerization:

$$-\ln(1-X) = 2\left(\frac{\bar{k}_p}{\bar{k}_t^{0.5}}\right)\left(\frac{2f[\mathrm{I}]_0}{\bar{k}_d}\right)^{0.5} \times\left[1 - \exp\left(\frac{-\bar{k}_d(t-\tau_I)}{2}\right)\right] \tag{6}$$

where τ_I is the induction time (min).

Kinetic models for thermal analysis

The overall kinetics of a thermal reaction can be expressed by the following lumped model:

$$\phi\frac{dX}{dT} = Af(X)\exp\left(-\frac{E}{RT}\right) \tag{7}$$

where A is the pre-exponential factor (1/min), E is the activation energy (J/mol), R is the universal gas constant, 8.314 J/gmole.K, T is the temperature, ϕ is the rate of heating ($\phi = dT/dt$), and $f(X)$ is the conversion function or reaction model. Integration of eq. (7) leads to the following integral isoconversional formulations:

$$\begin{aligned} F(X) &= \frac{A}{\phi}\int_0^T\left[\exp\left(-\frac{E}{RT}\right)\right]dT \\ &\equiv \frac{AE}{\phi R}p(x) \equiv \frac{A}{\phi}I(E,T) \end{aligned} \tag{8}$$

where $F(X) = \int_0^X \frac{dX}{f(X)}$, $x = \frac{E}{RT}$, $p(x)$ is the temperature integral, which cannot be exactly calculated, and $I(E,T)$ is a defined function of activation energy and temperatue. Instead, numerical values, series approximations, and other approximate expressions have been used.[33–38] Assuming $2RT < 1$, Coats and Redfern[39] suggested an asymptotic solution for the temperature integral as follows:

$$\ln\left(\frac{f(X)}{T^2(1-2RT/E)}\right) = \ln\left(\frac{AR}{\phi E}\right) - \left(\frac{E}{R}\right)\frac{1}{T} \tag{9}$$

Using different simplifying assumptions, Li and Tang[16,18] proposed another asymptotic solution for the temperature integral:

$$\ln\left(\frac{f(X)(1-6(RT/E)^2)}{T^2(1-2RT/E)}\right) = \ln\left(\frac{AR}{\phi E}\right) - \left(\frac{E}{R}\right)\frac{1}{T} \tag{10}$$

Also, Vyazovkin and coworkers[20–25] proposed a nonlinear isoconversional method based on the data of multiple ϕ values that takes into account the variation of E with the conversion:

$$\frac{I(E_X, T_{X,1})}{\phi_1} = \frac{I(E_X, T_{X,2})}{\phi_2} = \cdots = \frac{I(E_X, T_{X,n})}{\phi_n} \quad (11)$$

where E_x is activation energy as a function of conversion, and T_x is temperature as a function of conversion.

The estimation of E_X from this set of nonlinear algebraic equations is equivalent to the solution of the following minimization problem:

$$\min\left\{\sum_{i}^{n}\sum_{j\neq i}^{n}\left[\frac{I(E_X, T_{X,i})\phi_j}{I(E_X, T_{X,j})\phi_i}\right]\right\} \quad (12)$$

Estimation method

When the residual errors are normally distributed, it is known that the least square methods are optimal estimators for regression.[26,27] In the absence of normality, particularly when outliers are present in the data set, other more robust regression estimators have better properties. If an appropriate weighting scheme is chosen, *M*-estimators[27,28] behave entirely robustly to any types of outlying points. If an estimation model is represented by $y_i = g(x_i; \beta) + \varepsilon_i$, the general *M*-estimator minimizes the following objective function:

$$\sum_{i=1}^{n}\Gamma(\varepsilon_i) = \sum_{i=1}^{n}\Gamma(y_i - g(x_i;\beta)) \quad (13)$$

where function Γ provides the contribution of each residual to the objective function. Differentiation of the objective function with respect to the β coefficients and setting the partial derivatives to zero yield a system of equations for the β coefficients. Here, to model $\Gamma(\varepsilon_i)$, the Tukey bisquare (or biweight) estimator[29] with the following objective function is considered:

$$\Gamma(\varepsilon) = \begin{cases} \dfrac{\hat{\lambda}^2}{6}\left\{1 - \left[1 - \left(\dfrac{\varepsilon}{\hat{\lambda}}\right)^2\right]^3\right\} & \text{for} \quad |\varepsilon| \leq \hat{\lambda} \\ \dfrac{\hat{\lambda}^2}{6} & \text{for} \quad |\varepsilon| > \hat{\lambda} \end{cases} \quad (14)$$

where $\hat{\lambda}$ is a tuning constant, the smaller values of which produce more resistance to outliers. $\hat{\lambda}$ is generally picked to give reasonably high efficiency in the normal case; in particular, $\hat{\lambda} = 4.685\sigma$ for the bisquare (where σ is the standard deviation of the errors) produces 95% efficiency when the errors are normal and still offers protection against outliers. To calculate $\hat{\lambda}$, an estimate of σ is needed. Usually, a robust measure of spread is used in preference to σ. A common approach is to take σ = MAR/0.6745, where MAR is the median absolute of the residual.[27]

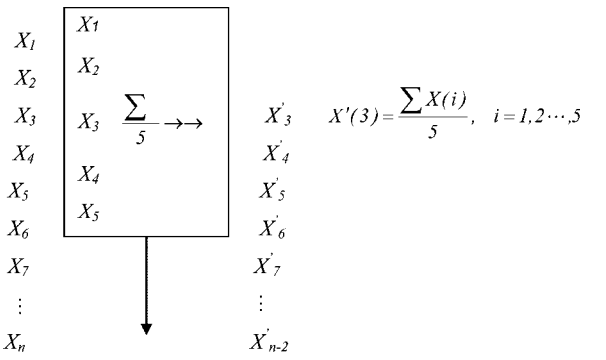

Figure 1 Concept of the moving average method for filtering noisy data (five-point average).

DETAILS OF COMPUTATION

Noise reduction from thermoanalysis data

Thermoanalysis data contain undesirable noise components that interfere with accurate extraction and interpretation of the desired data. These noisy data are often composed of high-frequency components that are greatly amplified by differentiation during data processing. It is assumed that the noise is random and normally distributed about the mean. The signal-to-noise ratio is defined as the ratio of the average signal magnitude to the root mean square of noise. Various methods including signal averaging, smoothing, and filtering in the frequency domain[40] are widely used to reduce the noise. Figure 1 shows the concept of the moving average method in the framework of smoothing methods. Convolution of a noisy TG or DSC curve with a filter is achieved by the filter function (ω) being pulled across the TG or DSC curve. The degree of smoothing is controlled by the number of points averaged (the width of the smoothing window). Mathematically, the output TG or DSC curve, X' (as an array), is the convolution product of the original TG curve, X, with ω:

$$X' = \omega \otimes X \quad (15)$$

A few mathematical manipulations are presented; their selection and tuning are somewhat empirical and depend on our application. Here, the techniques of Savitzky and Golay,[41] in which elements of ω can be obtained from the coefficients of a least square polynomial fit, are used.

Description of the computer program

An interactive computer program was written in C++, debugged, and executed on a Pentium IV 3.2-

GHz personal computer. Two options for data entry were considered: (1) interactive data entry and (2) reading the data from input data files. To retrieve the kinetic parameters from thermoanalysis data, a couple of model-dependent and model-free isoconversional methods were used. The estimation of kinetic parameters could be based on the complete set of data or flexible regional analysis. Three execution modes were available: (1) the model was assigned by the user, (2) the estimation was performed with all available models and the best model was selected on the basis of analysis of variance (ANOVA) tests, and (3) all models were solved and the results were sorted according to the correlation coefficient or *F*-statistic value.

EXPERIMENTAL

Materials

The initiator, 2,2′-azobisisobutyronitrile (AIBN; Fluka Chemica, Seelze, Germany; >98%), was crystallized three times from a mixture of chloroform and methanol below 40°C in subdued light. It was dried *in vacuo* at room temperature over P_2O_5 and stored in a dark place below −10°C until it was used. The monomers, i-BMA (Sigma-Aldrich, Munich, Germany; 99%) and LMA (Fluka; 98%), with 15 ppm methyl ethyl hydroquinone were washed three times with 10% NaOH and then three times with freshly distilled water, dried over $CaCl_2$, and distilled *in vacuo*. Copper stearate was used for peroxide breaking in a distillation chamber, and the middle fraction of the distillate was collected and dried *in vacuo* at room temperature over $CaCl_2$ and was stored at −10°C. The inhibitor DPPH was used without further purification. Benzene, used as a polymerization solvent, was distilled under nitrogen at reduced pressure. All other solvents and other reagents over the course of the thermoanalysis experiments and characterization were used as packaged without further purification.

Methods

DSC

DSC measurements were performed with a Mettler–Toledo (Zaventem, Belgium) DSC821 connected to a computer equipped with STAR V 6.0 evaluation software to manipulate and transfer the data. DSC was first calibrated in duplicate for the temperature and heat flow with the heats of fusion of several metals and by the measurement of the specific heat of synthetic sapphire over a wide range. The temperature axis was calibrated for each value of ϕ according to the calibration procedure of ASTM E 1582 with the same ϕ values, purge gas, and flow rate used for the samples. The DSC cell was swept by a constant flow of nitrogen at 20 mL/min. Isothermal tests were performed at 70°C, and nonisothermal tests were performed with ϕ values of 0.5, 1.0, 3.0, and 5.0°C/min.

All solution polymerizations were performed in benzene. For all experiments, an initial initiator concentration of 0.15 mol/L was used, whereas the concentration ratios of the inhibitor to the initiator were adjusted to 0.01, 0.05, 0.1, and 0.2. The polymerization mixture containing the monomers, solvent, inhibitor, and initiator was poured into vials and placed in a water bath at 15°C. Fresh solutions were prepared just before each set of experimental runs. Solutions were mixed vigorously with a magnetic stirrer until the initiator powder dissolved and a homogeneous solution was achieved. Vials were flushed with oxygen-free nitrogen for 10 min to remove the dissolved gases, subjected to three freeze–pump–thaw cycles to remove residual oxygen, and stored in a freezer. The DSC samples were prepared by the removal of a small amount of the frozen solution and its placement in an aluminum DSC pan, which was weighed and covered with an aluminum lid. The pan was sealed with a press and loaded into the DSC chamber. In the lid, a small hole was made so that decomposition products could escape. All sample sizes were less than 10 mg. An empty covered aluminum sample pan was used as the reference cell. Inert gas purging was maintained for a sufficient time to ensure that all residual oxygen was removed from the system before the reaction. Time was measured from the instant that the frozen sample pan was placed in the DSC instrument, and the sample–reference differential signal was recorded. The presence of an inhibitor caused an induction period to precede the onset of reaction. Once the polymerization was completed, the instrument was cooled, cleaned, and prepared for additional experiments.

TG

TG measurements were performed with a Mettler TA 3000 TG50 thermobalance. The sample preparation was the same as that for the DSC experiments. The temperature axis was calibrated with alumel, mumetal, and trafoperm, the Curie points of which were 149.00, 393.66, and 744.00°C, respectively. The temperature calibration was performed before every change in ϕ. The precision normally required implied the highest possible sensitivity on the temperature axis, which is usually 4°C/cm. About 5 mg of an AIBN sample was heated from 30 to about 150°C with ϕ values of 0.5, 1, 3, and 5°C/min. In general, a sample weight resulting in a maximum heat generation of less than 8 mJ/s was satisfactory. Before the start of the temperature program, samples were equilibrated at a temperature below the decomposition temperature. A nitrogen gas flow rate of 20 mL/min was considered to sweep away the decomposition products.

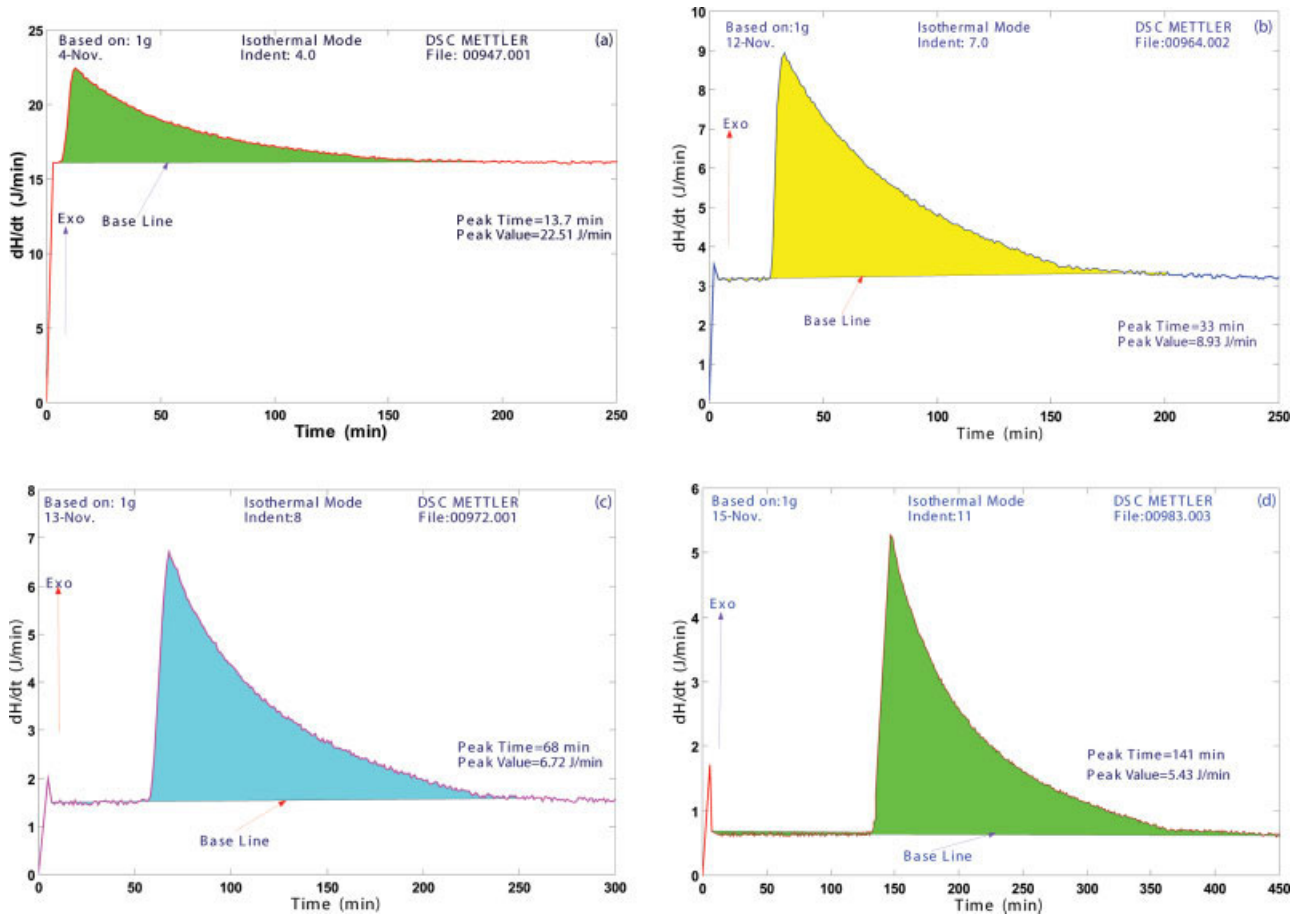

Figure 2 DSC curves for the copolymerization of i-BMA/LMA at f_{10} = 0.5 for different levels of $[z]_0/[I]_0$: (a) 0.01, (b) 0.05, (c) 0.1, and (d) 0.2. [Color figure can be viewed in the online issue, which is available at www.interscience.wiley.com.]

RESULTS AND DISCUSSION

Results of the DSC experiments

Inhibited polymerization

The *in situ* polymerization experiments were performed at 70°C and $[z]_0/[I]_0$ values of 0.01, 0.05, 0.1, and 0.2 (where [z] is the inhibitor concentration). The relevant DSC curves for f_{10} = 0.5 (where f_{10} is the molar fraction of i-BMA in the feed mixture at time zero) are shown in Figure 2(a–d), respectively. Isothermal measurements have the advantage of complete separation between the variables of time and temperature. The selection of an isothermal temperature equal to 70°C was based on the previous experimental studies for this copolymerization system.[1] The end of the inhibition period was determined by the intersection of the initial baseline with the tangent line drawn to the rising initial rate peak. The reaction reached completion when the DSC curve had fallen asymptotically to the initial baseline. The distance between the DSC curves and baseline was taken to be the instantaneous heat generation rate.

The noisy DSC curves were smoothed by a Savitzky–Golay convolution filter. The elements of the weight vector (ω) were obtained from the coefficients of the least square fit of the noisy data to a quadratic polynomial that was equal to ω = [−21, 14, 39, 54, 59, 54, 39, 14, −21]. For all DSC curves, setting the width of the smoothing window to at most 9 was adequate to remove all undesired noise components from the DSC curves.

In homopolymerization reactions, the rate of heat generation (Q_{gen}) is proportional to the rate of monomer consumption with the proportionality constant (ΔH_p), which is the total enthalpy of homopolymerization [$Q_{gen} = \Delta H_p \times R_p$, where R_p is the polymerization rate (mol/L min)]. In the case of copolymerization reactions, the situation is more complicated because instead of a single reaction, multiple elementary reactions are involved in the propagation step. The partial contribution of each propagation reaction to the overall heat generation changes with conversion because of compositional drift. Thus, the proportionality coefficient between Q_{gen} and R_p is not constant and varies with the conversion. To

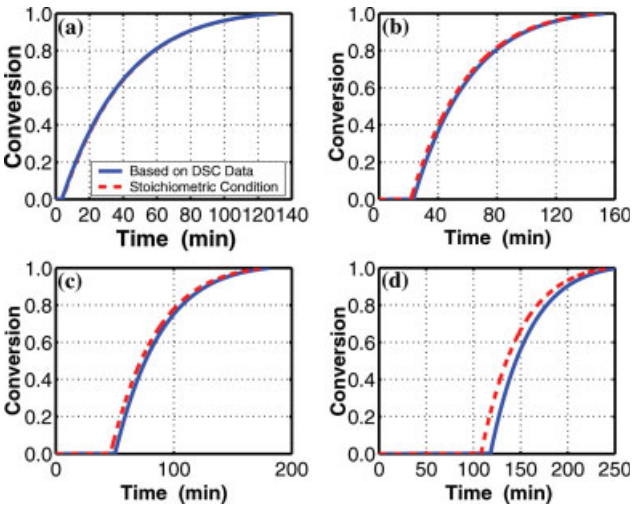

Figure 3 Conversion-time curves for i-BMA/LMA copolymerization at 70°C for different levels of $[z]_0/[I]_0$: (a) 0.01, (b) 0.05, (c) 0.1, and (d) 0.2. [Color figure can be viewed in the online issue, which is available at www.interscience.wiley.com.]

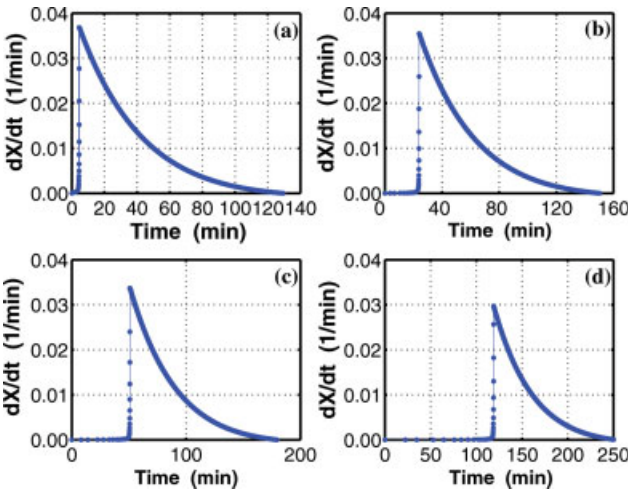

Figure 4 Calculated copolymerization rates for different levels of $[z]_0/[I]_0$: (a) 0.01, (b) 0.05, (c) 0.1, and (d) 0.2. [Color figure can be viewed in the online issue, which is available at www.interscience.wiley.com.]

remedy this problem, we first simply calculated the conversion at each reaction time from the corresponding partial areas of the DSC curves. Then, the overall reaction rate was calculated by numerical differentiation of the conversion data. With this calculation procedure, the variability of the proportionality coefficient between Q_{gen} and R_p was fully captured, and the limitations of the lumped method of analysis were overlooked.

The DSC curves were integrated with the Gauss–Legendre quadrature method,[42] and the extent of reaction was calculated with $X = (\int_{T_i}^{T} H(t,X)dt)/\Delta H_p$ and is shown in Figure 3. Here, $\int_{T_i}^{T} H(t,X)dt$ is the partial area under the DSC curve up to a certain time (the heat that evolved up to a certain time), and ΔH_p is the total heat of reaction. The results of the overall conversion were fitted to a polynomial with stepwise regression, and the rate of polymerization was subsequently calculated by numerical differentiation and is shown in Figure 4. As can be seen in this figure, caution must be taken in the assumption of a stationary state treatment near the end of the inhibition period because in such situations the radical concentration changes rapidly, and the steady-state assumption fails.

Because the induction period represents the required time for the consumption of primary radicals, its measurement provides a direct calculation of the *in situ* initiation rates. f was previously determined[43] by the mean kinetic chain length approach and was equal to 0.62. It was assumed that the efficiency of initiation was constant and was not influenced by the presence of the inhibitor. With the data of the induction period, the relevant kinetic parameters in eq. (5), that is, $\bar{k}_d$, $\overline{C}_Z$, and Ω, were determined by a robust *M*-estimation method. The resultant values are given in Table I. Because weights for leverage points were inserted in the estimation process, a robust procedure for all types of outliers was obtained. In the setup of the estimator, the addition of weights for leverage points was not computationally expensive because the estimators only needed to be scaled and orthogonally equivariant. To better quantify the sensitivity of the inhibited polymerization system toward the value of the stoichiometric ratio (Ω), the differential equation [eq. (5)] was numerically solved for $\Omega = 1.0$ (stoichiometric condition), and the predicted conversion is also shown in Figure 3. The predicted results for $\Omega = 1.0$ followed the same trend as the experimental conversion data from the DSC curves, but with a little bit of time lag. For all concentration ratios of the inhibitor to the initiator, the predicted conversions with $\Omega = 1.0$ were higher than the conversions from the DSC data. This was due to the higher values of estimated Ω; that is, increased initiator consumption during the inhibition period led to lower levels of available initiator for the uninhibited period, and finally a lower polymerization rate was attained. With the inhibitor/initiator ratio increasing, the differences between the two aforementioned curves in Figure 3 significantly increased. For each value of $[z]_0/[I]_0$, τ_I was also calculated with eq. (4) and is given in Table II. The predicted values of τ_I were in good agreement with the corresponding values in the DSC curves.

TABLE I
Kinetic Parameter Estimates for the Inhibition Period

$\bar{k}_d$ (min^{-1})	$\overline{C}_Z$	Ω
0.0021	1873	1.09

TABLE II
τ_I Values and Limiting Conversions in the Inhibition Period

$[z]_0/[I]_0$	τ_I (min)	Limiting conversion in the induction period
0.01	4.59	0.0171
0.05	23.96	0.0179
0.10	50.94	0.0191
0.20	118.87	0.0233

The total enthalpy of polymerization for different values of $[z]_0/[I]_0$ was calculated and is shown in Figure 5. The average heat of copolymerization was 61.02 kJ/mol. The dependence of the copolymerization heat on $[z]_0/[I]_0$ did not follow a definite trend.

To determine the variation of $\bar{k}_d$ and $\bar{k}_p/\bar{k}_t^{0.5}$ with the monomer feed composition, similar *in situ* DSC polymerization experiments for f_{10} values of 0.1, 0.3, 0.7, and 0.9 were performed. All experiments were carried out again at 70°C with only $[z]_0/[I]_0 = 0.05$. The relevant DSC curves followed the same trend as those presented in Figure 2; they are not shown here for the sake of brevity. For each initial monomer feed composition, the low conversion copolymerization data (<10% conversion) were extracted from the respective DSC curves and used for the estimation of the initiation and coupled rate parameters in eq. (6). Because the sampling time for the DSC experiments was 1 min, a huge set of data points participated in the estimation process, and much more confidence was attained with respect to other experimental methods such as gravimetry and densitometry. Furthermore, the propagated errors in the estimated parameters due to the experimental errors in sampling, fractionation, and characterization were removed.

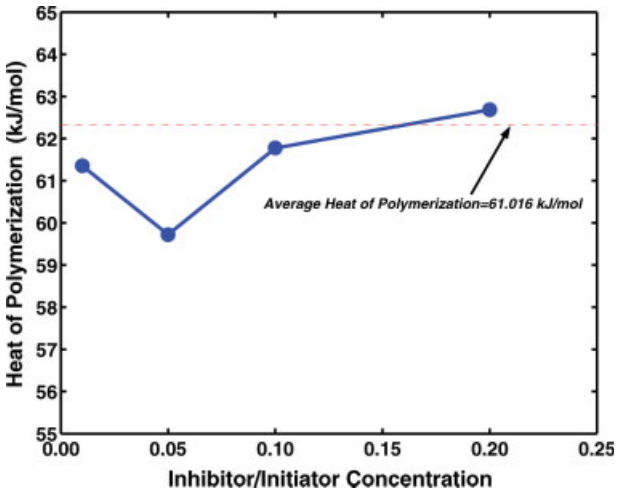

Figure 5 Overall heat of the copolymerization reaction at 70°C at $f_{10} = 0.5$ for different levels of $[z]_0/[I]_0$. [Color figure can be viewed in the online issue, which is available at www.interscience.wiley.com.]

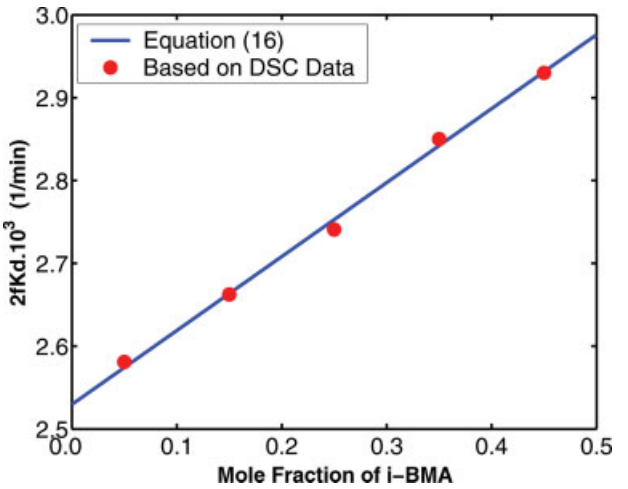

Figure 6 Variation of $2\overline{fk}_d$ with the molar fraction of i-BMA in the monomer phase ($f_{10} = 0.5$). [Color figure can be viewed in the online issue, which is available at www.interscience.wiley.com.]

To determine the compositional variation of $\bar{k}_p/\bar{k}_t^{0.5}$, it was assumed that $2\overline{fk}_d$ varies linearly with the monomer feed composition according to the following empirical relationship:[32]

$$2\,\overline{fk}_d = f_1(2\,fk_d)_1 + f_2(2\,fk_d)_2 \tag{16}$$

The estimated values of $2\overline{fk}_d$ at different monomer feed compositions were determined by robust *M*-estimation and are shown in Figure 6. If we assume a constant value of $f = 0.62$, the values of $\bar{k}_d$ vary from 2.08×10^{-3} to 2.36×10^{-3} min^{-1}, which is within the range of values reported in the literature.[2] Also, the values of the coupled rate parameter, $\bar{k}_p/\bar{k}_t^{0.5}$, at different monomer feed compositions were estimated and are shown in Figure 7. The solid line

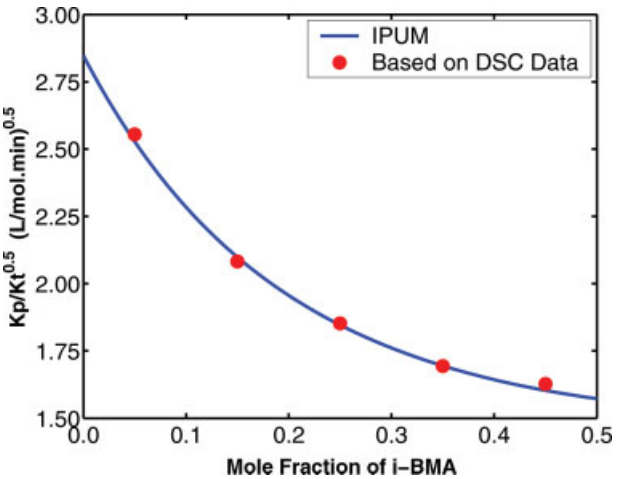

Figure 7 Variation of the coupled rate parameter, $\bar{k}_p/\bar{k}_t^{0.5}$, with the molar fraction of i-BMA in the monomer phase ($f_{10} = 0.5$). [Color figure can be viewed in the online issue, which is available at www.interscience.wiley.com.]

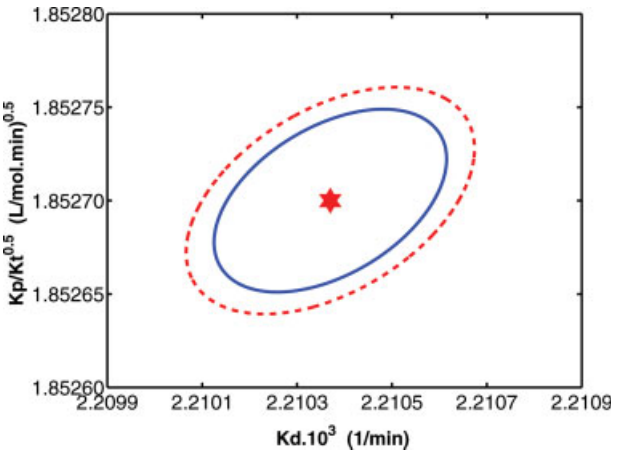

Figure 8 (—) 95% and (- - -) 99% JCRs for rate parameters estimated by robust *M*-estimation. [Color figure can be viewed in the online issue, which is available at www.interscience.wiley.com.]

in this figure shows the prediction of the implicit penultimate unit model (IPUM) of Fukuda and coworkers[44,45] with the reactivity ratios previously reported by Habibi and Vasheghani-Farahani.[43]

Joint confidence regions (JCRs) of $\bar{k}_d$ and $\bar{k}_p/\bar{k}_t^{0.5}$ for $f_{10} = 0.5$ were calculated for 95 and 99% probability levels and are shown in Figure 8. JCRs are ellipsoidal contours of a constant density, defined by K with probability α, such that $(K - \mu)' \sum^{-1} (K - \mu) \leq \chi^2_p, (1 - \alpha)$. These ellipsoids are centered at $\mu = [\bar{k}_d, \bar{k}_p/\bar{k}_t^{0.5}]$ and have axes of $\pm\sqrt{\chi^2_p \lambda_i \ell_i}$, where λ_i and ℓ_i are eigenvalues and eigenvectors of the variance–covariance matrix, respectively, and Σ is the variance–covariance matrix of parameter estimates. The small area of the JCRs indicates the high precision attained for kinetic parameters because of the good capability of the estimation method.

Similarly to $f_{10} = 0.5$, for each initial monomer feed composition, the DSC curves were integrated by the Gauss–Legendre quadrature method,[42] and the values of the overall heat of polymerization were calculated and are presented in Table III. In accordance with the results of Figure 7 for $\bar{k}_p/\bar{k}_t^{0.5}$, the overall heat of reaction decreased with the initial i-BMA molar fraction in the copolymerization system increasing, and this justified the higher polymerization rates for LMA-rich copolymers.

TABLE III
Variation of ΔH_p with f_{10}

f_{10}	ΔH_p (kJ/mol)
0.1	82.3
0.3	67.5
0.5	60.1
0.7	54.9
0.9	52.7

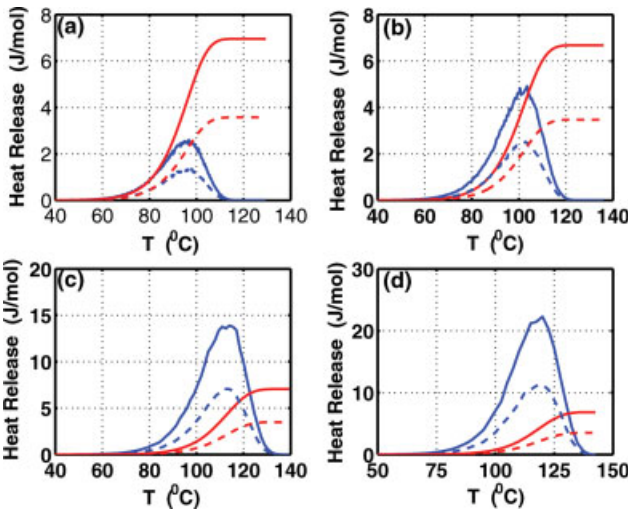

Figure 9 DSC curves for the decomposition of (—) unaged and (- - -) aged samples of AIBN at different values of ϕ: (a) 0.5, (b) 1.0, (c) 3.0, and (d) 5.0. The dark line shows instantaneous heat release, and the light line shows cumulative heat release. [Color figure can be viewed in the online issue, which is available at www.interscience.wiley.com.]

Initiator decomposition

The kinetics of initiator decomposition in the presence of a solvent were studied with nonisothermal DSC experiments with four different ϕ values (0.5, 1.0, 3.0, and 5.0°C/min). The resultant DSC curves are shown in Figure 9. Because DSC was first calibrated at 10°C/min, the nominal temperature readout for each ϕ value was corrected with the values in the operating manual of the Mettler–Toledo DSC821. Also, the thermal lag correction was calculated from thermal lag correction $(Tl_c) = \Pi \times Нь \times R_o$ imposed on DSC data. Here, Π is the instrument sensitivity (mw/cm), $Нь$ is the peak height (cm), and R_o is the thermal resistance (K/mw) of DSC. Similarly, the extent of reaction is defined as $X = (\int_{T_i}^{T} H(T)dt)/\Delta H_{\text{decomp}}$ (decomposition heat of initiator), where the integral in the numerator is the partial area under the DSC curve up to a certain temperature divided by the total.

TABLE IV
Arrhenius Parameters for AIBN Decomposition at Different Values of ϕ

ϕ (°C/min)	Log A (1/min)	E (kJ/mol)	R^2 statistic	F statistic
0.50	16.96	128.52	0.998	6,308,375.70
1.00	16.93	128.43	0.996	1,560,475.70
3.00	17.04	129.01	1.000	1,400,745.10
5.00	17.10	129.86	0.997	1,053,628.20

According to the overall data at various values of ϕ, log $A = 16.95$ min^{-1} and $E = 128.57$ kJ/mol.

TABLE V
Results of Aging Experiments for the Confirmation of DSC Results

ϕ (°C/min)	Aging temperature (°C)	Heat release (J/g)		Absolute error (%)
		Unaged sample	Aged sample	
0.50	82.54	6.97	3.53	1.17
1.00	82.81	7.12	3.75	5.31
3.00	83.78	7.07	3.76	6.36
5.00	84.81	6.82	3.65	7.03

ΔH_{decomp} = 228.23 kJ/mol; absolute error (%) = (unaged sample − 2 × aged sample) × 100/unaged sample.

Assuming first-order decomposition

$$\ln\left(\frac{1}{\Delta H_{decomp}}\frac{dH(T)}{dT}\right) = \ln A - \left(\frac{E}{R}\right)\frac{1}{T} + \ln\left(\frac{\Delta H_{decomp} - H(T)}{\Delta H_{decomp}}\right) \quad (17)$$

where $dH(t)/dt$ is the rate of heat evolution. The greatest advantage of DSC is providing a direct measure of the instantaneous rate of reaction rather than the conversion. The conversion is readily calculated from integration of the rate data. This procedure is inherently more accurate than evaluating rates from numerical differentiation of the conversion data. A high value of ϕ may allow some of the sample to melt before it decomposes, whereas with a low value of ϕ, the entire reaction occurs below the melting temperature. On the other hand, the use of low values of ϕ allow us to narrow the temperature range of a nonisothermal experiment, and this may help us to conduct the isothermal and nonisothermal experiments over comparable ranges of temperatures and reduce the quantitative difference between the dependences of E on the extent of the reaction derived from isothermal and nonisothermal experiments.

With the corrected thermoanalysis data, the Arrhenius parameters of initiator decomposition were calculated by robust M-estimation, and the results are given in Table IV. The F statistics in Table IV refer to the values of the F test in statistical tables with 95% confidence. With ϕ increasing, the values of F statistics of estimation decrease. Thus, more reliable kinetic parameters can be obtained from thermoanalysis experiments at lower ϕ values.

To verify the accuracy of the decomposition rate parameters in Table IV, isothermal aging experiments were designed. For each sample, an aging time equal to 60 min was considered, and it was assumed that the aging time was equal to the half-life of the initiator ($t_{1/2}$). Then, the corresponding aging temperature was calculated from $t_{1/2} = 0.693/\bar{k}_d$ with the estimated kinetic parameters in Table IV. The samples were aged isothermally at that temperature and quenched immediately to a temperature at least 50°C below the aging temperature. Therefore, no significant reaction occurred during the subsequent holding time. The aged samples were subjected to DSC under the same temperature program used for the unaged sample, and the TG curves were recorded and compared with that of the unaged one in Figure 9. On an equal weight basis, the peak area of an aged sample should be one half that of an unaged sample. The verification analysis is given in Table V. Again, with ϕ increasing, the absolute error of estimation increased. The average value of ΔH_{decomp} in the presence of a solvent was also calculated to be 228.23 kJ/mol.

Results of the TG experiments

Similarly to DSC, the noisy TG curves were smoothed by a Savitzky–Golay convolution filter and are shown in Figure 10. The observed spikes around 105°C for ϕ values of 0.5 and 1°C/min may be due to domination of the buoyancy effect in TG instrumentation. The fractional conversion (X) is defined

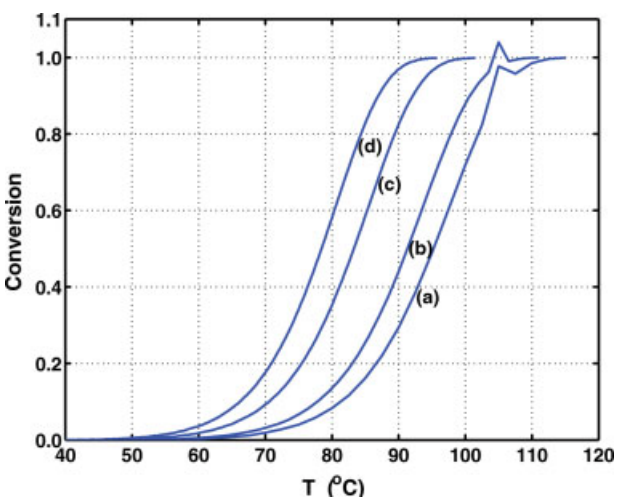

Figure 10 Smoothed TG curves for the decomposition of AIBN in the temperature range of 40–120°C: (a) ϕ = 0.5°C/min, (b) ϕ = 1°C/min, (c) ϕ = 3°C/min, and (d) ϕ = 5°C/min. [Color figure can be viewed in the online issue, which is available at www.interscience.wiley.com.]

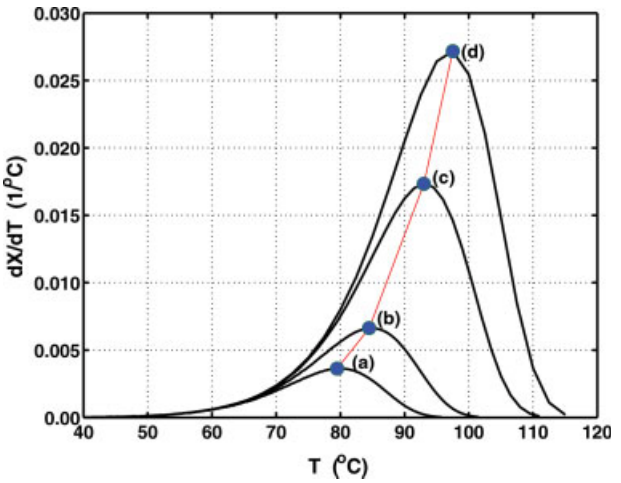

Figure 11 Effect of ϕ on the thermal decomposition rate of AIBN: (a) ϕ = 0.5°C/min, (b) ϕ = 1°C/min, (c) ϕ = 3°C/min, and (d) ϕ = 5°C/min. [Color figure can be viewed in the online issue, which is available at www.interscience.wiley.com.]

as follows:

$$X = \frac{W_e}{W_0 - W_f} = \frac{W_0 - W_r - W_f}{W_0 - W_f} = 1 - \frac{W_r}{W_0 - W_f} \quad (18)$$

where W_0 is the initial weight, W_e is the evolved gas weight, W_r is the reactive weight, and W_f is the final nonreactive weight. The effect of different ϕ values on the maximum decomposition rate is also shown in Figure 11. With ϕ increasing, the maximum decomposition rate increased, and the locus of the maximum rate shifted to higher temperatures. These experimental data were used to test several phenomenological kinetic models.

The estimated parameter values along with the statistics of estimation for the models of Coats and Redfern[39] and Li and Tang[18] are given in Table VI. The estimated values of A and E show global overprediction with respect to their DSC counterparts in Table IV. The order of the F statistic values for DSC-based estimates is 10^2 times higher than that of the TG-based estimates. Both methods use Arrhenius integral approximation. Although the values of the F statistics for the Li–Tang model[18] are larger than those of the Coats–Redfern model,[39] no significant differences between the results were obtained. The calculated values of $\bar{k}_d$ from both DSC and TG experiments were higher than the resultant values from the inhibition polymerization experiments in Table I, possibly because of the cage recombination effect in the polymerization media.

An ANOVA for the model of Li and Tang[18] was performed with 432 extracted data points. The results in Table VII indicate that the sum of squares of the residual was smaller than the sum of squares of the estimation, and this indicated the adequacy of the model and goodness of fit attained with robust M-estimators.

The dependence of E on the extent of reaction was found by the implementation of nonlinear numerical optimization of the model of Vyazovkin[25] [eq. (12)]. The resultant values are shown in Figure 12. The average value of E is 140.10 kJ/mol, and its variation with conversion is significant. If we observe a strong dependence of E on conversion, different model-fitting methods yield different values of E. The isoconversional method predicts a lower degree of decomposition for long periods of time in comparison with any of the model-fitting methods. The model of Vyazovkin removes the systematic errors due to the approximation of the temperature integral. As a result, the model-free method predicts a lower decomposition rate for long periods of time in comparison with any of the standard model-fitting methods.

CONCLUSIONS

The solution copolymerization kinetics of i-BMA/LMA have been studied by the design of a set of *in situ* inhibited polymerization experiments with DSC. The kinetic parameters of copolymerization have been retrieved with a robust M-estimation method. This has indicated that robust M-estimation can outperform existing methods of estimation in terms of statistical precision and computational speed, while keeping good robustness properties. The major conclusions are as follows:

- In comparison with the classical methods of experimental kinetics, only small amounts of a sample are needed; the propagated errors in the estimated parameters due to sampling, fractionation, and characterization are removed; and the rate parameters as well as the heat of reaction can be obtained from a single run. Thus, thermo-

TABLE VI
Results of Robust *M*-Estimation for AIBN Decomposition Using Nonisothermal TG Data

Kinetic model	log A (1/min)	E (kJ/mol)	Correlation coefficient	F statistic
Coats–Redfern	19.09	142.57	−0.986	15,261
Li–Tang	18.60	139.75	−0.953	17,141

TABLE VII
ANOVA Table of *M*-Estimation for the Model of Li and Tang

Model	Sum of squares	Degree of freedom	Mean square	F_{cal}
Estimation	3428.27	1	3428.27	17,141
Residual	86.60	432	0.20	
Total	3514.87	433		

$$SSE = \sum_{i=1}^{N}\left[(X_i)_{exp} - \left(\sum_{i=1}^{N}(X_i)_{exp}\right)/N\right]^2$$

$$SSR = \sum_{i=1}^{N}[(X_i)_{pred} - (X_i)_{exp}]^2$$

$MSE = SSE/p$

$MSR = SSR/(N\text{-}p)$

$F_{cal} = MSE/MSR$

MSE = mean square of the estimation; MSR = mean square of the residual; N = number of data points; SSE = sum of squares of the estimation; SSR = sum of squares of the residual.

P, degree of freedom in the estimation model.

analysis methods are likely to become an interesting alternative for the kinetic study of polymerization systems.

- The calculation procedure allows us to fully capture the variability of the instantaneous copolymerization heat with the conversion and skip the limitations of lumped methods of analysis.
- The dependence of the coupled rate parameter, $\bar{k}_p/\bar{k}_t^{0.5}$, on the monomer feed composition is well represented by IPUM of Fukuda and coworkers.[44,45] The small areas of JCRs for $\bar{k}_d$ and $\bar{k}_p/\bar{k}_t^{0.5}$ show reasonable precision for estimated kinetic parameters. The high values of F statistics indicate the robustness of the M-estimation method.
- The calculated values of $\bar{k}_d$ from both DSC and TG experiments are higher than the resultant value from inhibition polymerization experiments, possibly because of the presence of a cage recombination effect in the polymerization media.
- The isoconversional method allows us to consider the variation of E with the conversion and predicts a lower degree of decomposition for long periods of time in comparison with any of the model-fitting methods. The use of a model-free isoconversional approach is recommended as a trustworthy way of obtaining reliable and consistent Arrhenius kinetics from thermoanalysis data.

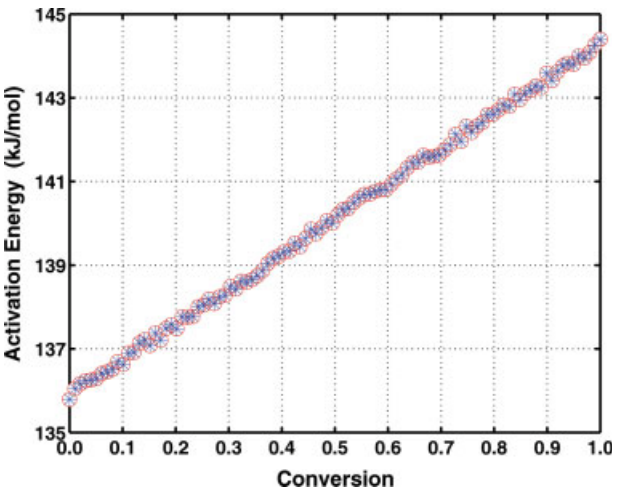

Figure 12 Variation of the activation energy with the conversion for the thermal decomposition of AIBN. [Color figure can be viewed in the online issue, which is available at www.interscience.wiley.com.]

NOMENCLATURE

Symbols

A	pre-exponential factor (1/min)
C_Z	inhibition parameter $\bar{k}_z/\bar{k}_p$)
E	activation energy (J/mol)
f	initiator efficiency
$f(X)$	conversion function
f_i	molar fraction of monomer i in the feed mixture
f_{10}	molar fraction of i-BMA in the feed mixture at time zero
[I]	initiator concentration (mol/L)
$\bar{k}_d$	decomposition rate parameter of the initiator (1/min)
$\bar{k}_i$	initiation rate parameter (L/mol min)
$\bar{k}_p$	propagation rate parameter (L/mol min)
$\bar{k}_t$	termination rate parameter (L/mol min)
$\bar{k}_{tc}$	termination by combination rate parameter (L/mol min)
$\bar{k}_{td}$	termination by disproportionation rate parameter (L/mol min)
$\bar{k}_{tr}$	transfer to solvent rate parameter (L/mol min)
$\bar{k}_z$	inhibition rate parameter (L/mol min)

$\bar{k}_{zp}$	reinitiation rate parameter (L/mol min)
$\bar{k}_{zt}$	annihilation rate parameter (L/mol min)
ℓ_i	eigenvector of the variance–covariance matrix of parameter estimates
[M]	overall monomer concentration (mol/L)
N	number of data points
$p(x)$	temperature integral
Q_{gen}	heat generation (J/min)
R_i	initiation rate (mol/L min)
R_o	thermal resistance (K/mw)
R_p	polymerization rate (mol/L min)
t	polymerization time (min)
$t_{1/2}$	half-life of the initiator (min)
W_0	initial weight
W_e	evolved gas weight
W_f	final nonreactive weight
W_r	reactive weight
X	fractional or overall conversion
X	original data in thermogravimetric curves
X'	output data from thermogravimetric curves
[z]	inhibitor concentration (mol/L)

Greek symbols

Ь	peak height (cm)
α	probability level
Γ	function providing the contribution of each residual to the objective function
ΔH_p	total heat of polymerization (J/mol)
λ_i	eigenvalue of the variance-covariance matrix of parameter estimates
$\hat{\chi}$	tuning parameter for the estimator
Π	instrument sensitivity (mw/cm)
ρ	density of the polymerization system
σ	standard deviation of the errors
Σ	variance-covariance matrix of parameter estimates
σ^2	variance of estimation
τ_I	induction time (min)
ϕ	heating rate (°C/min)
ω	array of weights in a Savitzky–Golay convolution filter
Ω	stoichiometric ratio

References

1. Habibi, A.; Mahabadi, P. Optimization of Reaction Conditions for Viscosity Index Improvers; RIPI Internal Report; Tehran, Iran, 2002.
2. Brandrup, J.; Immergut, E. H.; Grulke, E. A. Polymer Handbook, 4th ed.; Wiley: New York, 1999.
3. Paulik, F. Special Trends in Thermal Analysis; Wiley: Chichester, England, 1995; Chapter 10.
4. Kessler, M. R.; White, S. R. J Polym Sci Part A: Polym Chem 2002, 40, 2373.
5. Horie, K. J Polym Sci Part A-1: Polym Chem 1970, 8, 1357.
6. Sebastian, D. H.; Biesenberger, J. A. J Appl Polym Sci 1979, 23, 661.
7. Rehak, A.; Tudos, F. Eur Polym J 1980, 16, 241.
8. Sestak, J. J Therm Anal 1979, 16, 503.
9. Flynn, J. H. J Therm Anal 1983, 27, 95.
10. Urbanovici, E.; Segal, E. Thermochim Acta 1985, 91, 373.
11. Urbanovici, E.; Segal, E. Thermochim Acta 1985, 94, 257.
12. Urbanovici, E.; Segal, E. Thermochim Acta 1985, 95, 271.
13. Urbanovici, E.; Segal, E. Thermochim Acta 1986, 107, 339.
14. Agrawal, P. K. Thermochim Acta 1992, 203, 93.
15. Flynn, J. H. Thermochim Acta 1997, 300, 83.
16. Li, C. R.; Tang, T. B. J Therm Anal 1997, 49, 1243.
17. Li, C. R.; Tang, T. B. Thermochim Acta 1999, 325, 43.
18. Li, C. R.; Tang, T. B. J Mater Sci 1999, 34, 3467.
19. Flynn, J. H. J Therm Anal 1991, 37, 293.
20. Vyazovkin, S.; Linert, W. Chem Phys 1995, 193, 109.
21. Vyazovkin, S.; Linert, W. Int Rev Phys Chem 1995, 14, 355.
22. Vyazovkin, S. Int J Chem Kinet 1996, 28, 95.
23. Vyazovkin, S.; Dollimore, D. J Chem Inf Comput Sci 1996, 36, 42.
24. Vyazovkin, S. J Therm Anal 1997, 49, 1493.
25. Vyazovkin, S. J Comput Chem 1997, 18, 393.
26. Wakeling, I. N.; MacFie, H. J. H. J Chemometr 1992, 6, 189.
27. Rousseeuw, R. J.; Leroy, A. M. Robust Regression and Outlier Detection; Wiley: New York, 1987.
28. Huber, P. J. Ann Math Stat 1964, 35, 73.
29. Cummins, D. J.; Andrews, C. Chemometr J 1995, 9, 489.
30. Tobita, H.; Hamielec, A. E. Polymer 1991, 32, 2641.
31. O'Driscoll, K. F.; Huang, J. Eur Polym J 1989, 25, 629.
32. Fernandez-Garcia, M.; Madruga, E. L. J Polym Sci Part A: Polym Chem 1997, 35, 1961.
33. Dowdy, D. R. J Therm Anal 1987, 32, 1177.
34. Budrugeac, P.; Petre, A. L.; Segal, E. J Therm Anal 1996, 47, 123.
35. Popescu, C. Thermochim Acta 1996, 285, 309.
36. Sbirrazzuoli, N.; Girault, Y.; Elegant, L. Thermochim Acta 1997, 293, 25.
37. Budrugeac, P.; Segal, E. J Therm Anal 1998, 53, 441.
38. Budrugeac, P.; Segal, E. J Min Metall 1999, 35, 187.
39. Coats, A. W.; Redfern, J. P. Nature 1964, 201, 68.
40. Hori, K. J Polym Sci Part A-1: Polym Chem 1964, 7, 254.
41. Savitzky, A.; Golay, M. Anal Chem 1964, 36, 1627.
42. Nakamura, S. Applied Numerical Methods with Software; Prentice-Hall: London, 1991.
43. Habibi, A.; Vasheghani-Farahani, E. Macromol Theory Simul 2004, 13, 520.
44. Fukuda, T.; Ma, Y. D.; Inagaki, H. Macromolecules 1985, 18, 17.
45. Fukuda, T.; Kubo, K.; Ma, Y. D. Prog Polym Sci 1992, 17, 875.